

Isolation and Crystallographic Characterization of $\text{ErSc}_2\text{N@C}_{80}$: an Endohedral Fullerene Which Crystallizes with Remarkable Internal Order

Marilyn M. Olmstead,[†] Ana de Bettencourt-Dias,[†] J. C. Duchamp,^{‡,§} S. Stevenson,^{‡,⊥} Harry C. Dorn,^{*,‡} and Alan L. Balch^{*,†}

Contribution from the Department of Chemistry, University of California, Davis, California 95616 and the Department of Chemistry, Virginia Polytechnic Institute and State University, Blacksburg, Virginia 24061

Received June 5, 2000

Abstract: The $\text{Er}_n\text{Sc}_{3-n}\text{N@C}_{80}$ ($n = 0-3$) family of four endohedral fullerenes has been prepared by vaporization of graphite rods packed with 2% $\text{Sc}_2\text{O}_3/3\%$ $\text{Er}_2\text{O}_3/95\%$ graphite powder in a Krätschmer–Huffman fullerene generator under dynamic flow of helium and dinitrogen. $\text{ErSc}_2\text{N@C}_{80}$ has been isolated in pure form via three stages of high-pressure liquid chromatography and characterized by mass spectrometry. The first structure of a mixed metal endohedral, $\text{ErSc}_2\text{N@C}_{80}$, has been determined by single-crystal X-ray diffraction at 90 K on $\text{ErSc}_2\text{N@C}_{80}\cdot\text{Co}^{\text{II}}(\text{OEP})\cdot 1.5\text{C}_6\text{H}_6\cdot 0.3\text{CHCl}_3$, which was obtained by diffusion of a solution of $\text{ErSc}_2\text{N@C}_{80}$ in benzene into a solution of $\text{Co}^{\text{II}}(\text{OEP})$ (OEP is the dianion of octaethylporphyrin) in chloroform. The structure of $\text{ErSc}_2\text{N@C}_{80}$ consists of a planar ErSc_2N unit surrounded by an icosahedral C_{80} cage. The nominal Er–N distance is 2.089(9) Å and the Sc–N distance is, as expected, shorter, 1.968(6) Å. Despite its location within the C_{80} cage, the ErSc_2N unit displays a remarkable degree of order within the solid-state structure. The metal ions make close contact with individual carbon atoms of the cage with shortest Sc–C distances, in the range of 2.03–2.12 Å, and shortest Er–C distances of 2.20 and 2.22 Å. Two different, but equally populated, orientations of the I_hC_{80} cage were required to describe the fullerene portion of the structure. Although these C_{80} cages are located on a crystallographic mirror plane, that plane does not coincide with a mirror plane of the cages themselves. Consequently, the cage is disordered over four superimposed sites.

Introduction

The original recognition¹ of the unique stability of C_{60} was rapidly followed by news that metal ions could be incorporated into the central portion of fullerene cages to produce a family of endohedral fullerenes such as La@C_n .² However, progress in exploring the chemical and physical properties of the endohedral fullerenes has been slowed by three factors: the low yields in which most endohedrals are produced, the frequent low solubility of the endohedrals, and the air sensitivity of some of these species. Nevertheless, many endohedrals have been detected with one, two, or three atoms, generally electropositive metal atoms, incorporated within the carbon cages, which range in size from U@C_{28} ³ to $\text{La}_3\text{@C}_{106}$ and beyond.⁴ Two recent reviews of the field are available.^{5,6}

Recently the preparation of the novel endohedral, $\text{Sc}_3\text{N@C}_{80}$, which contains the planar tetra-atomic Sc_3N unit within the fullerene cage has been reported.^{7,8} This novel endohedral is formed by conducting the normal Krätschmer–Huffman arc fullerene preparation with scandium oxide-doped graphite rods in a dynamic atmosphere that contains dinitrogen in addition to helium. This process, the trimetallic nitride template (TNT) method, produces $\text{Sc}_3\text{N@C}_{80}$ in an abundance which exceeds that of C_{84} , the most prevalent of the fullerenes with masses greater than C_{70} , and makes macroscopic quantities of $\text{Sc}_3\text{N@C}_{80}$ available for chemical and physical characterization. $\text{Sc}_3\text{N@C}_{80}$ has been characterized by ¹³C, ¹⁴N, and ⁴⁵Sc NMR spectroscopy, UV/vis spectroscopy, and by a single-crystal X-ray diffraction study of the cocrystallized solid, $\text{Sc}_3\text{N@C}_{80}\cdot\text{Co}^{\text{II}}(\text{OEP})\cdot 0.5\text{C}_6\text{H}_6\cdot 1.5\text{CHCl}_3$ (OEP is the dianion of octaethylporphyrin).^{9,10,11} Although the crystallographic work revealed the

[†] University of California, Davis.

[‡] Virginia Polytechnic Institute and State University.

[§] Permanent address: Emory and Henry College, Emory, Virginia, 24327-0943.

[⊥] Permanent address: Luna Nanomaterials, 2851 Commerce Street, Blacksburg, VA 24060.

(1) Kroto, H. W.; Heath, J. R.; O'Brien, S. C.; Curl, R. F.; Smalley, R. E. *Nature* **1985**, *318*, 162.

(2) Heath, J. R.; O'Brien, S. C.; Zhang, Q.; Liu, Y.; Curl, R. F.; Kroto, H. W.; Tittel, F. K.; Smalley, R. E. *J. Am. Chem. Soc.* **1985**, *107*, 7779.

(3) Guo, T.; Diener, M. D.; Chai, Y.; Alford, M. J.; Hauffler, R. E.; McClure, S. M.; Ohno, T.; Weaver, J. H.; Scuseria, G. E.; Smalley, R. E. *Science* **1992**, *257*, 1661.

(4) Alvarez, M. M.; Gillan, E. G.; Holczer, K.; Kaner, R. B.; Min, K. S.; Whetten, R. L. *J. Phys. Chem.* **1991**, *95*, 10561.

(5) Shinohara, H. In *Fullerenes: Chemistry, Physics, and Technology*; Kadish, K. M., Ruoff, R. S., Eds. John Wiley and Sons: New York, 2000, p 357.

(6) Nagase, S.; Kobayashi, K.; Akasaka, T.; Wakahara, T. In *Fullerenes: Chemistry, Physics, and Technology*; Kadish, K. M., Ruoff, R. S., Eds. John Wiley and Sons: New York, 2000, p 395.

(7) Stevenson, S.; Rice, G.; Glass, T.; Harich, K.; Cromer, F.; Jordan, M. R.; Craft, J.; Hadju, E.; Bible, R.; Olmstead, M. M.; Maitra, K.; Fisher, A. J.; Balch, A. L.; Dorn, H. C. *Nature* **1999**, *401*, 55.

(8) Dorn, H. C.; Stevenson, S.; Craft, J.; Cromer, F.; Duchamp, J.; Rice, G.; Glass, T.; Harich, K.; Fowler, P. W.; Heine, T.; Hajdu, E.; Bible, R.; Olmstead, M. M.; Maitra, K.; Fisher, A. J.; Balch, A. L. Proceedings of the IWEPNM2000 Conference; Kirchberg/Tyrol, Austria, March 4–10, 2000; American Institute of Physics; in press.

(9) Crystallization of fullerenes is frequently accompanied by orientational disorder, which impedes detailed structural study. However, cocrystallization of fullerenes with $\text{Co}^{\text{II}}(\text{OEP})$ and other porphyrins produces crystals in which the fullerene frequently is ordered or sufficiently ordered to allow analysis of its structure.^{10,11}

location of the Sc_3N unit within the fullerene cage, residual electron density in the vicinity of the cage indicated that one or more alternative cage orientations were present, but this aspect of disorder was unresolved.

The empty-cage fullerenes, C_{80} along with C_{74} and C_{72} , have been considered as "missing fullerenes" because of their low abundances in raw fullerenes soot and/or in raw soot extract.¹² Seven isomeric structures of the C_{80} cage [with symmetries D_2 , D_{5d} , C_{2v} , C_{2v}' (two distinct isomers), D_3 , D_{5h} , and I_h] fulfill the isolated pentagon rule.¹³ Theoretical calculations indicate that these idealized structures have open shell structures and are subject to Jahn–Teller effects, which lower their symmetries.¹⁴ The empty cage C_{80} isomers D_2 and D_{5d} (D_5) are nearly equal in energy and are the most stable isomers. The stability of the entire range of C_{80} isomers decreases in the following order: D_2 and D_{5d} (D_5) > C_{2v} > C_{2v}' (C_s) > D_3 (C_3) > D_{5h} (C_s) > I_h (D_2), where the lowered symmetry of the affected cages is given in parentheses. Two forms of the empty cage C_{80} have been isolated and identified as the D_2 and D_{5d} isomers on the basis of their ^{13}C NMR spectra.^{15,16}

Despite the low intrinsic abundance of C_{80} in fullerene extracts, the formation of endohedral fullerenes by the standard Krätschmer–Huffman technique has provided access to several other C_{80} -based endohedrals including $\text{La}_2@C_{80}$, $\text{Pr}_2@C_{80}$,¹⁷ $\text{Ce}_2@C_{80}$,¹⁸ and $\text{M}@C_{80}$ ($\text{M} = \text{Ca}, \text{Sr}, \text{Ba}$).¹⁹ Sufficient quantities of $\text{La}_2@C_{80}$ have been purified and isolated so that a number of spectroscopic,²⁰ electrochemical,²¹ and chemical properties²² of this endohedral fullerene have been explored. Electronic structure calculations have shown that the stability of the I_h of isomer of C_{80} increases markedly when six electrons are added to the cage to provide a closed-shell electronic structure.^{23,24} As a result, the I_h isomer becomes the most stable structure for $(C_{80})^{-6}$.²⁵ For $\text{La}_2@C_{80}$, calculations reveal that the I_h structure is favored with a formal $(\text{La}^{3+})_2(C_{80})^{6-}$ electron distribution within the molecule. The ^{13}C and ^{139}La NMR spectra of solutions of $\text{La}_2@C_{80}$ have been interpreted in terms of an I_h structure for the C_{80} , with the metal atoms undergoing rapid circular motion within the carbon cage.²⁰ Similarly, the spec-

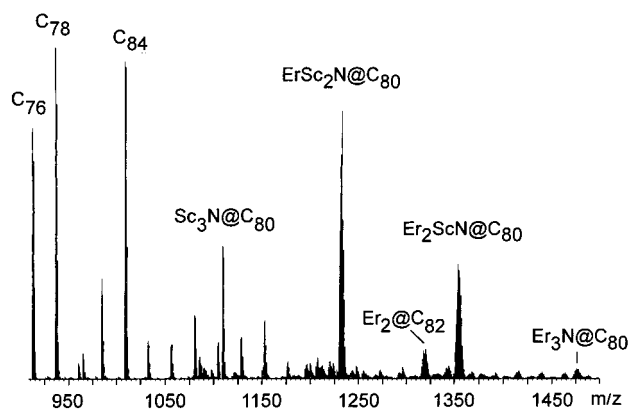


Figure 1. Mass spectrum of the raw CS_2 extract that was utilized to obtain $\text{ErSc}_2\text{N}@C_{80}$. The intense mass clusters due to C_{60} and C_{70} are not shown.

troscopic and crystallographic data on $\text{Sc}_3\text{N}@C_{80}$ are consistent with the presence of a carbon cage with I_h symmetry for which the $(\text{Sc}^{3+})_3(\text{N}^{3-})@(C_{80}^{6-})$ electronic distribution is probable.⁷

Here we report the preparation of the $\text{Er}_n\text{Sc}_{3-n}\text{N}@C_{80}$ ($n = 0-3$) family of endohedrals, the isolation of $\text{ErSc}_2\text{N}@C_{80}$, and its detailed structural characterization by single-crystal X-ray diffraction.

Results and Discussion

Synthesis of the $\text{Er}_n\text{Sc}_{3-n}\text{N}@C_{80}$ ($n = 0-3$) Family and Isolation and Characterization of $\text{ErSc}_2\text{N}@C_{80}$. Vaporization of graphite rods packed with 2% $\text{Sc}_2\text{O}_3/3\%$ $\text{Er}_2\text{O}_3/95\%$ graphite powder (with cobalt^{II} oxide as a catalyst) in a Krätschmer–Huffman fullerene generator under dynamic flow of helium and dinitrogen produces a black soot. Extraction of this raw soot with cold carbon disulfide produces a reddish-orange solution of soluble empty cage and metal encapsulated fullerenes. A portion of the mass spectrum obtained from the material in the carbon disulfide extract is shown in Figure 1. Mass clusters arising from the presence of the $\text{Er}_n\text{Sc}_{3-n}\text{N}@C_{80}$ family are present in the following order of decreasing abundance: $\text{ErSc}_2\text{N}@C_{80} > \text{Er}_2\text{ScN}@C_{80} > \text{Sc}_3\text{N}@C_{80} > \text{Er}_3\text{N}@C_{80}$. In addition, the customary peaks due to C_{76} , C_{78} , and C_{84} are seen along with those of $\text{Er}_2@C_{82}$. The intense features coming from the more abundant C_{60} and C_{70} molecules are not shown.

$\text{ErSc}_2\text{N}@C_{80}$ was isolated from the raw soot and purified via three stages of high-pressure liquid chromatography (HPLC). The first stage utilized a pentabromobenzyl column with carbon disulfide as eluant and an automated HPLC procedure that has been outlined previously.²⁶ The C_{84} – C_{88} fraction from the pentabromobenzyl column was then collected and further separated using a Buckyclutcher column with a toluene mobile phase. To remove coeluting impurities in this fraction, a third round of HPLC utilized a Buckyprep column with toluene as eluant. The final HPLC trace is shown in Figure 2, along with the mass spectrum obtained from this sample. $\text{ErSc}_2\text{N}@C_{80}$ forms reddish-brown solutions in carbon disulfide and benzene which are stable to air. Although the overall yield of $\text{ErSc}_2\text{N}@C_{80}$ represents 3–5% of the total soluble extract (see Figure 1), it is very difficult to remove the TNT endohedral metallofullerenes ($\text{Er}_3\text{N}@C_{80}$ and $\text{ScEr}_2@C_{80}$) impurities because of chromatographic coelution with very similar elution times on the Buckyprep column. Nevertheless, from 10 packed graphite rods, 150 mg of soluble extract was obtained and 1–2 mg of purified $\text{ErSc}_2\text{N}@C_{80}$ was recovered.

(10) Olmstead, M. M.; Costa, D. A.; Maitra, K.; Noll, B. C.; Phillips, S. L.; Van Calcar, P. M.; Balch, A. L. *J. Am. Chem. Soc.* **1999**, *121*, 7090.

(11) Boyd, P. D. W.; Hodgson, M. C.; Rickard, C. E. F.; Oliver, A. G.; Chaker, L.; Brothers, P. J.; Bolskar, R. D.; Tham, F. S.; Reed, C. A. *J. Am. Chem. Soc.* **1999**, *121*, 10487.

(12) Wan, T. S. M.; Zhang, W.; Nakane, T.; Xu, M.; Inakume, H.; Shinohara, H.; Kobayashi, K.; Nagase, S. *J. Am. Chem. Soc.* **1998**, *120*, 6806.

(13) Fowler, P. W.; Manolopoulos D. E. *An Atlas of Fullerenes*. Oxford University Press: Oxford, 1995; p 254.

(14) Kobayashi, K.; Nagase, S.; Akasaka, T. *Chem. Phys. Lett.* **1995**, *245*, 230.

(15) Hennrich, F. H.; Michel, R. H.; Fischer, A.; Richard-Schneider, S.; Gilb, S.; Kappes, M. M.; Fuchs, D.; Bürk, M.; Kobayashi, K.; Nagase, S. *Angew. Chem., Int. Ed. Engl.* **1996**, *35*, 1732.

(16) Wang, C.-R.; Sugai, T.; Kai, T.; Tomiyama, T.; Shinohara, H. *Chem. Commun.* **2000**, 557.

(17) Ding, J.; Yang, S. *J. Am. Chem. Soc.* **1996**, *118*, 11254.

(18) Ding, J.; Yang, S. *Angew. Chem., Int. Ed. Engl.* **1996**, *35*, 2234.

(19) Dennis, T. J. S.; Shinohara, H. *Chem. Commun.* **1998**, 883.

(20) Akasaka, T.; Nagase, S.; Kobayashi, K.; Wälchli, M.; Yamamoto, K.; Funasaka, H.; Kako, M.; Hoshino, T.; Erata, T. *Angew. Chem., Int. Ed. Engl.* **1997**, *36*, 1643.

(21) Suzuki, T.; Maruyama, Y.; Kato, T.; Kikuchi, K.; Nakao, Y.; Achiba, Y.; Kobayashi, K.; Nagase, S. *Angew. Chem., Int. Ed. Engl.* **1995**, *34*, 4, 1094.

(22) Akasaka, T.; Nagase, S.; Kobayashi, K.; Suzuki, T.; Kato, T.; Kikuchi, K.; Achiba, Y.; Yamamoto, K.; Funasaka, H.; Takahashi, T. *Angew. Chem., Int. Ed. Engl.* **1995**, *34*, 2139.

(23) Fowler, P. W. *Chem. Phys. Lett.* **1986**, *131*, 444.

(24) Gillan, E. G.; Yeretizian, C.; Min, K. S.; Alvarez, M. M.; Whetten, R. L.; Kaner, R. B. *J. Phys. Chem.* **1992**, *96*, 6869.

(25) Fowler, P. W.; Zerbetto, F. *Chem. Phys. Lett.* **1995**, *243*, 36.

(26) Stevenson, S.; Dorn, H. C.; Burbank, P.; Harich, K.; *Anal. Chem.* **1994**, *66*, 2675.

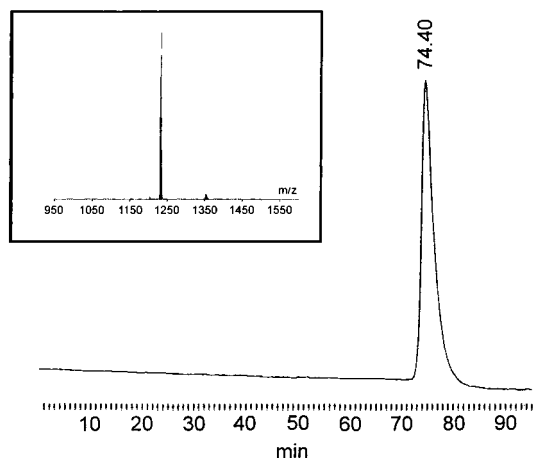


Figure 2. The HPLC trace for the purified sample of $\text{ErSc}_2\text{N}@C_{80}$ utilized in this work. The insert shows the mass spectrum of this sample.

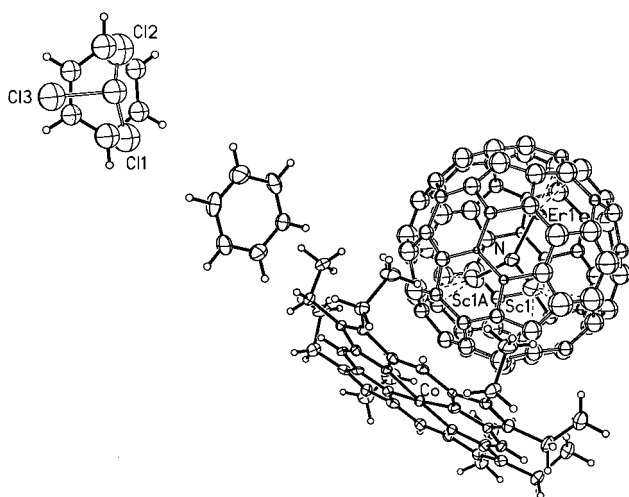


Figure 3. Perspective view of the independent molecules and their relative orientations within crystalline $\text{ErSc}_2\text{N}@C_{80}\cdot\text{Co}^{\text{II}}(\text{OEP})\cdot 1.5\text{C}_6\text{H}_6\cdot 0.3\text{CHCl}_3$ with 50% thermal contours for all non-hydrogen atoms. Only one orientation of the C_{80} cage is shown. The site on the left is partially occupied by chloroform and benzene, which are shown superimposed.

Crystallization and Structural Analysis of $\text{ErSc}_2\text{N}@C_{80}\cdot\text{Co}^{\text{II}}(\text{OEP})\cdot 1.5\text{C}_6\text{H}_6\cdot 0.3\text{CHCl}_3$. Because the sample of $\text{ErSc}_2\text{N}@C_{80}$ itself did not appear to form X-ray diffraction quality crystals, cocrystallization with $\text{Co}^{\text{II}}(\text{OEP})$ ^{9,10} was attempted and found to yield a suitable material: $\text{ErSc}_2\text{N}@C_{80}\cdot\text{Co}^{\text{II}}(\text{OEP})\cdot 1.5\text{C}_6\text{H}_6\cdot 0.3\text{CHCl}_3$. Figure 3 shows the individual molecular components of the solid and their relative orientations. The solid consists of five independent molecules that occupy four sites. One site, which is shown in the upper left of Figure 3, is fractionally occupied by a molecule of benzene and a molecule of chloroform. Figure 4 shows a stereo diagram that illustrates the molecular packing within the solid.

$\text{ErSc}_2\text{N}@C_{80}$. The $\text{ErSc}_2\text{N}@C_{80}$ molecule sits at a site of crystallographic mirror symmetry. However, the C_{80} cage itself is orientationally disordered, and none of the 15 mirror planes of any one of the icosahedral cages coincides with the crystallographic mirror plane.^{27,28} Figure 5 presents a stereo drawing which shows the two orientations of the cages

(27) Other cases in which the fullerene does not utilize the crystallographic site symmetry are known. For example, in $\text{C}_{60}\cdot 5\text{Ag}(\text{NO}_3)$ the C_{60} cage resides at a site of *mm* symmetry but is disordered over four orientations.

(28) Olmstead, M. M.; Maitra, K.; Balch, A. L. *Angew. Chem., Int. Ed. Engl.* **1999**, *38*, 231.

superimposed upon one another. Because of this disorder in the cage, it was necessary to refine it as a rigid group using idealized coordinates. In this model, the C–C bond distances at 6:6 ring junctions are held at 1.4263 Å, while the C–C bond distances at 6:5 ring junctions are 1.4276 Å. This model produces a C_{80} cage with an 8.19-Å diameter between carbon atoms at the junction of two six-membered rings and one five-membered ring and an 8.133-Å diameter between carbon atoms that join three six-membered rings. Because the C_{80} cage was disordered and treated as a rigid group, it was not possible to determine whether the incorporation and localization of the ErSc_2N unit within the cage produced any distortion of the cage.

Figure 6 presents information about the ErSc_2N group and its relationship to the cage around it. Part a shows the ErSc_2N group alone. The N and Er atoms lie on a crystallographic mirror plane. The nominal Er–N distance is 2.089(9) Å and the Sc–N distance is, as expected, shorter, 1.968(6) Å. The Er–N–Sc angle is 119.1(3)° and the Sc–N–Sc angle is 121.3(6)°. The ErSc_2N unit is planar within experimental error, with the sum of the two Er–N–Sc angles and the Sc–N–Sc angle equal to 359.6°. The Er and Sc thermal ellipsoids are elongated in directions which are indicative of motion of the ErSc_2N group along the walls of the C_{80} cage. RMS analysis of the thermal motion compensates for this distortion and indicates that the range for the Er–N bond length is 2.09–2.20 Å, and the range for the Sc–N bond length is 1.97–2.06 Å.²⁹ The nominal nonbonded Sc···Sc and Sc···Er distances are 3.50 and 3.43 Å, respectively.

Parts b and c of Figure 6 show the relationships between the ErSc_2N group and the C_{80} cage surrounding it. Because there are two orientations of the C_{80} cage within the crystal, there are also two slightly different molecules of $\text{ErSc}_2\text{N}@C_{80}$ produced by coupling these cage orientations with the ErSc_2N portion. These molecules differ in regard to the interactions of the metal ions with the cage. Figures 7 and 8 show projections of the metal ions onto the inner surface of the C_{80} cages of the two distinct molecules. As it is seen in these drawings, each metal ion resides close to a single carbon atom of the cage, with Sc–C distances in the range 2.03–2.12 Å and Er–C distances of 2.20 and 2.22 Å. In molecule 1, shown in Figure 7, all of the metal atoms reside near carbon atoms that are located at the intersection of two hexagons and one pentagon. In molecule 2, as shown in Figure 8, the Er atom and one of the Sc atoms also lie over carbon atoms that are located at the intersection of two hexagons and one pentagon, but the other Sc atom lies over a carbon atom that resides at the intersection of three hexagons. Thus, the arrangement of scandium ions over carbon atoms is statistical. Within the icosahedral C_{80} cage, there are 60 carbon atoms that reside at the intersection of two hexagons and one pentagon, but there are only 20 carbon atoms that reside at the intersection of three hexagons.

In addition to the major site for the ErSc_2N group discussed above, examination of difference electron density maps during refinement indicated that there were other, less populated sites for the ErSc_2N group within the C_{80} cage. The ErSc_2N group shown in Figure 6 has a fractional occupancy of 0.80. In addition there are three sites of electron density, one on the crystallographic mirror plane, the others in general positions, which have been assigned to erbium atoms. Three other sites of lesser electron density in general positions within the cage have been assigned as scandium atoms. All of these sites are roughly 1.9–2.1 Å from the central nitrogen atom and are close to the

(29) Johnson, C. K. *Crystallographic Computing*; Munksgaard: Copenhagen, 1970; p. 220.

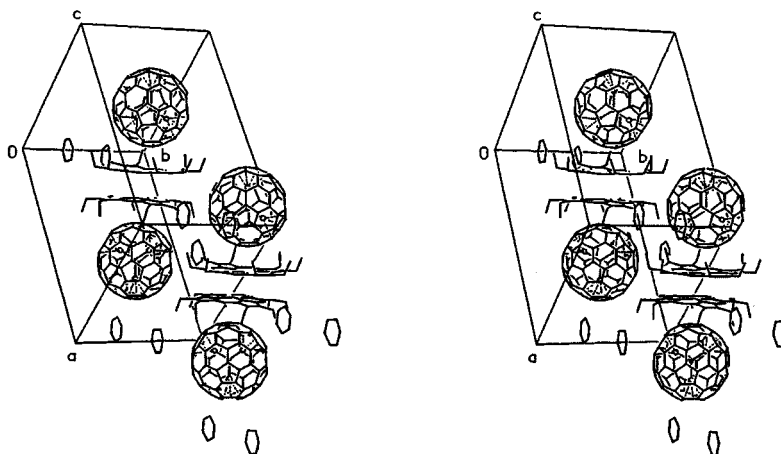


Figure 4. View of unit cell of $\text{ErSc}_2\text{N}@C_{80}\cdot\text{Co}^{\text{II}}(\text{OEP})\cdot 1.5\text{C}_6\text{H}_6\cdot 0.3\text{CHCl}_3$ which shows crystallographic packing of the components. Only one orientation of the C_{80} cage is shown, and the disordered chloroform is not shown.

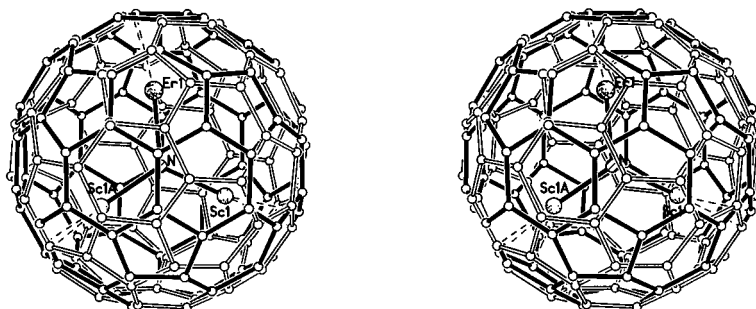


Figure 5. Drawing which shows a superposition of the two orientations of the C_{80} cage in $\text{ErSc}_2\text{N}@C_{80}\cdot\text{Co}^{\text{II}}(\text{OEP})\cdot 1.5\text{C}_6\text{H}_6\cdot 0.3\text{CHCl}_3$. One cage is shown with a solid line connecting the carbon atoms (small circles); the other cage orientation has open lines connecting the carbon atoms.

fullerene cage. All can be assembled into planar ErSc_2N units that resemble the ErSc_2N unit shown in Figure 6, but each of these has a different orientation within the cage (see supporting information).

$\text{Co}^{\text{II}}(\text{OEP})$ and Its Interaction with $\text{ErSc}_2\text{N}@C_{80}$ and Itself. The $\text{Co}^{\text{II}}(\text{OEP})$ molecule resides on a crystallographic mirror plane which coincides with a molecular mirror plane that bisects the cobalt atom, N(1), and N(3). The geometry of the $\text{Co}^{\text{II}}(\text{OEP})$ molecule is entirely normal. The Co–N distances [Co–N(1), 1.969(8); Co–N(2), 1.985(6); and Co–N(3), 1.976(7) Å] in $\text{ErSc}_2\text{N}@C_{80}\cdot\text{Co}^{\text{II}}(\text{OEP})\cdot 1.5\text{C}_6\text{H}_6\cdot 0.3\text{CHCl}_3$ are similar to those in $\text{Co}^{\text{II}}(\text{OEP})$ [Co–N, 1.967(3), 1.975(2) Å],³⁰ in $\text{C}_{60}\cdot 2\text{Co}^{\text{II}}(\text{OEP})\cdot \text{CHCl}_3$ [Co–N, 1.954(5)–1.985(6) Å], and in $\text{C}_{70}\cdot \text{Co}^{\text{II}}(\text{OEP})\cdot \text{C}_6\text{H}_6\cdot \text{CHCl}_3$ [Co–N, 1.964(5)–1.967(5) Å].¹⁰

The $\text{Co}^{\text{II}}(\text{OEP})$ molecule is positioned so that the ethyl groups of the porphyrin form an octapoidal embrace about the fullerene and the porphyrin plane is adjacent to the C_{80} cage. The fullerene is too far from the cobalt atoms for any normal covalent bonding between them. The closest approaches of the cobalt atom to the C_{80} cage involves C(9B), which is 2.706 Å from the cobalt atom, and C(78A), which is 2.746 Å from the cobalt atom. Although these distances are too long to represent true η^2 -coordination,³¹ they are shorter than the normal van der Waals contact seen between graphite layers (3.4 Å),³² between adjacent porphyrins (3.2 Å and larger),³³ and between neighboring fullerenes (>3.2 Å).^{34,35} The shorter Fe– C_{60} contact (Fe–C

distance, 2.63 Å) in $[\text{Fe}(\text{TTP})(\text{C}_{60})]^+$ has been described as having a covalent Fe–C interaction that is somewhat different from symmetrical η^2 -bonding.³⁶

In addition to these fullerene–porphyrin interactions, there are significant porphyrin–porphyrin contacts with pairwise, face-to-face contact. As is the case with $\text{C}_{60}\cdot 2\text{Co}^{\text{II}}(\text{OEP})\cdot \text{CHCl}_3$ and with $\text{C}_{70}\cdot \text{Co}^{\text{II}}(\text{OEP})\cdot \text{C}_6\text{H}_6\cdot \text{CHCl}_3$, the face-to-face porphyrin–porphyrin contact is greater in the fullerene cocrystals than it is in pristine $\text{Co}^{\text{II}}(\text{OEP})$ itself. Thus, the lateral shift (LS, 1.534 Å), mean plane separation (MPS, 2.994 Å), and the $\text{Co}\cdots\text{Co}$ separation (3.364 Å) in $\text{ErSc}_2\text{N}@C_{80}\cdot\text{Co}^{\text{II}}(\text{OEP})\cdot 1.5\text{C}_6\text{H}_6\cdot 0.3\text{CHCl}_3$ are shorter than the corresponding distances in $\text{Co}^{\text{II}}(\text{OEP})$ (LS, 3.38 Å; MPS, 3.33 Å, $\text{Co}\cdots\text{Co}$ separation, 4.742 Å) but are similar to those in $\text{C}_{70}\cdot\text{Co}^{\text{II}}(\text{OEP})\cdot\text{C}_6\text{H}_6\cdot\text{CHCl}_3$ (with LS, 1.67 Å; MPS, 3.19 Å, $\text{Co}\cdots\text{Co}$ separation, 3.392 Å). This close face-to-face arrangement in $\text{ErSc}_2\text{N}@C_{80}\cdot\text{Co}^{\text{II}}(\text{OEP})\cdot 1.5\text{C}_6\text{H}_6\cdot 0.3\text{CHCl}_3$ is facilitated by the positioning of all of the ethyl groups on the opposite side of the porphyrin plane from the adjacent $\text{Co}^{\text{II}}(\text{OEP})$ molecule. In contrast, $\text{Co}^{\text{II}}(\text{OEP})$ alone has four ethyl groups on one side of the porphyrin plane and four on the opposite side.³⁰

Discussion

The TNT approach has been successfully utilized to prepare the set of four endohedrals, $\text{Er}_n\text{Sc}_{3-n}\text{N}@C_{80}$ ($n = 0-3$). In the process described here, the raw soot that was obtained is particularly rich in the mixed metal species, $\text{ErSc}_2\text{N}@C_{80}$, which has been separated and isolated in pure form.

(30) Scheidt, W. R.; Turowska-Tyrk, I. *Inorg. Chem.* **1994**, *33*, 1314.

(31) Balch, A. L.; Olmstead, M. M. *Chem. Rev.* **1998**, *98*, 2123.

(32) Pauling, L. *The Nature of the Chemical Bond*, 3rd ed.; Cornell University Press: Ithaca, NY, 1960; p 260.

(33) Scheidt, W. R.; Lee, Y. J. *Struct. Bonding (Berlin)* **1987**, *64*, 1.

(34) Bürgi, H. B.; Restori, R.; Schwarzenbach, D.; Balch, A. L.; Lee, J. W.; Noll, B. C.; Olmstead, M. M. *Chem. Mater.* **1994**, *6*, 1325.

(35) Balch, A. L.; Lee, J. W.; Noll, B. C.; Olmstead, M. M. *J. Chem. Soc., Chem. Commun.* **1993**, 56.

(36) Evans, D. R.; Fackler, N. L. P.; Xie, Z.; Rickard, C. E. F.; Oliver, A. G.; Chaker, L.; Brothers, P. J.; Bolskar, R. D.; Boyd, P. D. W.; Reed, C. A. *J. Am. Chem. Soc.* **1999**, *121*, 8466.

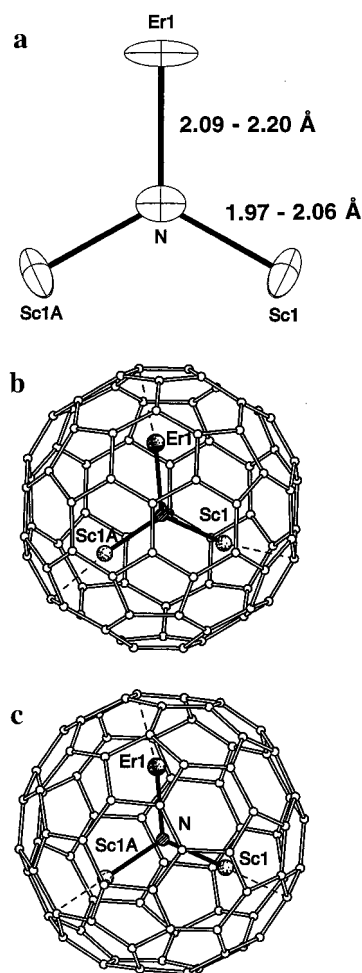


Figure 6. Drawings which show (a) the ErSc_2N unit alone with thermal ellipsoids, and b and c, the two molecules of $\text{ErSc}_2\text{N}@C_{80}$ (without thermal ellipsoids) which arise due to the cage disorder. In b and c, the dashed lines connect the metal ions to the nearest carbon atoms.

The crystallographic data indicate that the ErSc_2N unit is tightly packed within the C_{80} cage, because the Sc–N and Er–N distances, along with the shortest Sc–C and Er–C distances, are all shorter than the shortest comparable bond lengths in other compounds that these metal ions form. Moreover, these distances are (>0.25 Å) shorter than comparable mean bond lengths given in the Cambridge Structural Data Base (CSD).³⁷ The nominal Sc–N distance in $\text{ErSc}_2\text{N}@C_{80}$ is 1.968(6) Å, but a search of the CSD reveals that the mean Sc–N distance is 2.251 Å in 82 observed examples and that the previous shortest Sc–N distance was 2.039 Å (for dichloro-bis(tetrahydrofuran)-bis(trimethylsilyl)amido-scandium).³⁸ Other relevant comparisons include tris(bis(dimethylsilyl)amido)(tetrahydrofuran)-scandium with Sc–N distances of 2.063(2), 2.064(2), and 2.079(2) Å³⁹ and (η^5 -cyclopentadienyl)(octaethylporphyrin)scandium with an average Sc–N distance of 2.190(2) Å.⁴⁰ Similarly, the nominal Er–N distance in $\text{ErSc}_2\text{N}@C_{80}$ is 2.089(9) Å, but the mean Er–N distance in the CSD is 2.411 Å in 128 observed examples, and the previous shortest Er–N distance was 2.151 Å (for bis(μ_2 -triphenylphosphineiminato)-tris(η^5 -cyclopentadienyl)-(tri-

(37) Allen, F. H.; Davies, J. E.; Johnson, O. J.; Kennard, O.; Macrae, C. F.; Mitchell, E. M.; Mitchell, G. F.; Smith, J. M.; Watson, D. *J. Chem. Inf. Comput. Sci.* **1991**, *31*, 187.

(38) Karl, K.; Sybert, G.; Massa, W.; Dehnicke, K. *Z. Anorg. Allg. Chem.* **1999**, *625*, 375.

(39) Anwender, R.; Runte, O.; Eppinger, J.; Gerstberger, G.; Herdtweck, E.; Spiegler, M. *J. Chem. Soc., Dalton Trans.* **1998**, 847.

(40) Arnold, J.; Hoffman, C. G. *J. Am. Chem. Soc.* **1990**, *112*, 8620.

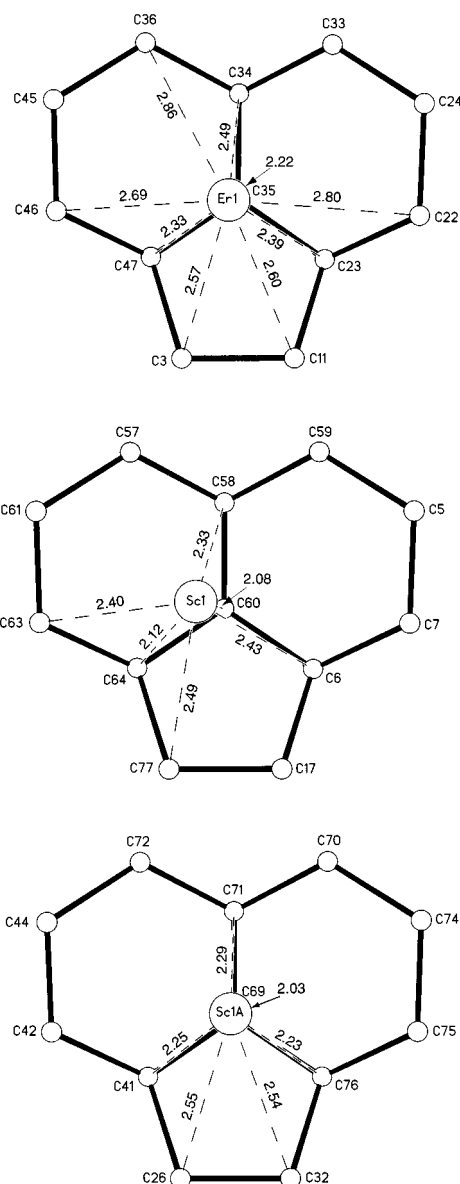


Figure 7. Projections which show the positions of the metal ions with respect to the adjacent walls of the C_{80} cage for one orientation of the cage (molecule 1).

phenylphosphineimino)-di-erbium).⁴¹ In a particularly relevant comparison, the average Er–N distance in [tetrakis(tetrahydrofuran)lithium]-[tetrakis(diphenylamido)erbium] is 2.26 Å.⁴² Similar considerations pertain to the shortest Sc–C and Er–C distances inside the cage. Thus, the shortest Sc–C distances in $\text{ErSc}_2\text{N}@C_{80}$ range from 2.029 to 2.121 Å, but the mean Sc–C distance is 2.430 Å in 73 examples in the CSD, and the shortest Sc–C distance in the CSD is 2.204 Å for the σ -Sc–C bond in bis(trimethylsilylmethyl)-*N,N*-bis(di-isopropylphosphinomethyl)dimethylsilylamido)-scandium.⁴³ In other relevant examples, the average Sc–C distance in (η^5 -cyclopentadienyl)(octaethylporphyrin)scandium is 2.494(4) Å,³⁹ and the average Sc–C distance in di-(μ -chloro)-bis(di- η^5 -cyclopentadienyl)scandium is 2.46 Å.⁴⁴ Similarly, the shortest Er–C distances in $\text{ErSc}_2\text{N}@C_{80}$ are

(41) Anfang, S.; Harms, K.; Weller, F.; Borgmeier, O.; Lueken, H.; Schilder, H.; Dehnicke, K. *Z. Anorg. Allg. Chem.* **1998**, *624*, 159.

(42) Wong, W.-K.; Zhang, L.; Xue, F.; Mak, T. C. W. *Polyhedron*, **1997**, *16*, 2013.

(43) Fryzuk, M. D.; Giesbrecht, G.; Rettig, S. J. *Organometallics*, **1996**, *15*, 3329.

(44) Atwood, J. L.; Smith, K. D. *J. Chem. Soc., Dalton Trans.* **1973**, 2487.

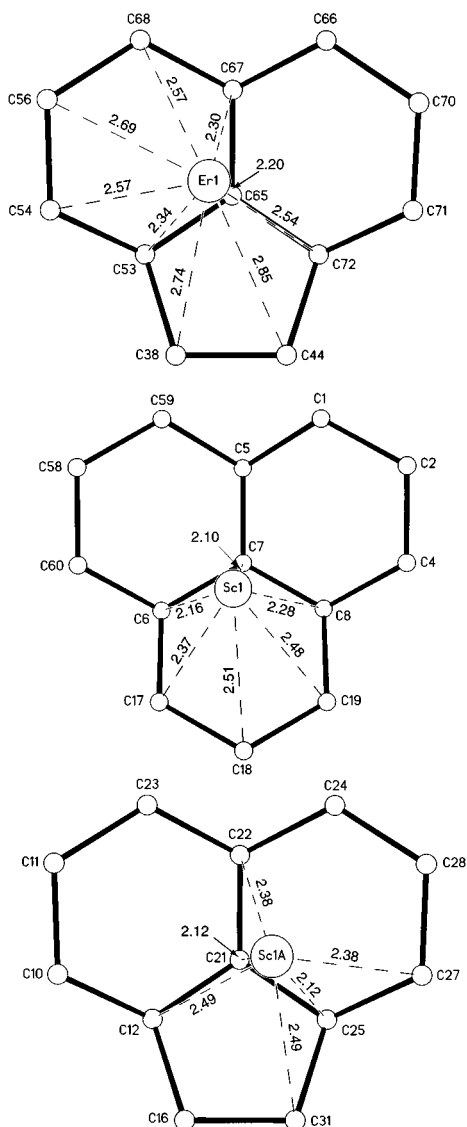


Figure 8. Projections which show the positions of the metal ions with respect to the adjacent walls of the C_{80} cage for the other orientation of the cage (molecule 2).

2.195 and 2.215 Å, but the mean Er–C distance in the CSD is 2.769 Å, and the shortest Er–C distance is 2.412 Å (in triphenyltris(tetrahydrofuran)-erbium),⁴⁵ and for comparison, the average Er–C distance in di- μ -chloro-bis(di- $(\eta^5\text{-cyclopentadienyl})\text{erbium}$) is 2.59 Å.⁴⁶ In considering the comparison of these M–C distances, it is important to realize that the orientation of the M–C unit in $\text{ErSc}_2\text{N@C}_{80}$ differs significantly from that in conventional π -bonded ligands, such as $\eta^5\text{-cyclopentadienyl}$ groups. In $\text{ErSc}_2\text{N@C}_{80}$, the metals reside near single carbon atoms, whereas in $(\eta^5\text{-C}_5\text{H}_5)$ complexes, which are particularly numerous in the CSD, the metal is centered over the cyclopentadienide ring, and consequently for such compounds the M–C distances are naturally longer than they would be if the metal were located directly over a single carbon atom.

The positions of the scandium atoms within the fullerene cage in $\text{ErSc}_2\text{N@C}_{80}$ can also be compared to structural information obtained from theoretical calculations and from the analysis of X-ray powder diffraction data on related scandium endohedral

complexes. Ab initio molecular orbital and density functional calculations have placed the Sc atoms 2.358 Å from the nearest carbon atoms in $\text{Sc}_2\text{@C}_{84}$ ⁴⁷ and 2.322 Å from the closest carbon atoms in $\text{Sc}_2\text{@C}_{80}$.⁴⁸ These are longer distances than those observed in $\text{ErSc}_2\text{N@C}_{80}$. However, fewer atoms are present in the interior of $\text{Sc}_2\text{@C}_{84}$ and $\text{Sc}_2\text{@C}_{80}$ than in $\text{ErSc}_2\text{N@C}_{80}$. Room temperature X-ray powder diffraction data have been analyzed for $\text{Sc}_3\text{@C}_{82}$ by a combination of Rietveld and maximum entropy method (MEM) methods.⁴⁹ The results produced a model in which an equilateral triangle of scandium atoms with a $\text{Sc}\cdots\text{Sc}$ distance of 2.3(3) Å resides within a C_{82} cage having C_{3v} symmetry and with the Sc atom 2.52(2) Å from the closest carbon atom of the C_{82} cage. A similar analysis of X-ray powder diffraction data for $\text{Sc}_2\text{@C}_{84}$ indicated that the $\text{Sc}\cdots\text{Sc}$ distance is 3.9(1) Å and that the shortest $\text{Sc}\cdots\text{C}$ contact is 2.4(2) Å.⁵⁰ Again the $\text{Sc}\cdots\text{C}$ contacts observed in $\text{ErSc}_2\text{N@C}_{80}$ are shorter.

Bonding within $\text{ErSc}_2\text{N@C}_{80}$ can be considered to consist of four components. First, there is the covalent C–C bonding that forms the cage itself. This cage then mechanically entraps the ErSc_2N unit. In addition to the mechanochemical encapsulation, there is a strong ionic component to the bonding in the endohedral. The $\text{ErSc}_2\text{N@C}_{80}$ molecule can be thought in formal terms to consist of three concentric rings of charge starting with the core nitride (N^{3-}), which is surrounded by three M^{3+} ions, which are then encapsulated by the $(\text{C}_{80})^{6-}$ cage. This formal charge distribution utilizes the characteristic M^{3+} oxidation state for both scandium and erbium and places a 6– charge on the C_{80} cage. These added electrons on the fullerene uniquely stabilize the I_h symmetry cage structure relative to the six other isomeric C_{80} cage geometries, as noted earlier.^{23,24} Given the close contacts inside the cage, there is no doubt significant orbital overlap that leads to covalent interactions among the components and to sharing of electron density so that the effective charges on the individual components are reduced below those given by the formal ionic model.

Although the ErSc_2N unit is firmly ensconced within the fullerene cage, it is also likely to be able to ratchet around inside the cage. The nature of the thermal ellipsoids shown in part A of Figure 7 is suggestive of such motion. The observation of additional, less populated sites of electron density within the cage also indicates that there are alternative locations for the group and again suggests that this group is able to move within the fullerene cage. The mobility of atoms within fullerenes cages has been suggested previously from NMR studies on $\text{La}_2\text{@C}_{80}$,²⁰ $\text{Sc}_3\text{N@C}_{80}$,⁷ $\text{Sc}_2\text{@C}_{84}$,⁵¹ and from EPR studies on $\text{Sc}_3\text{@C}_{82}$.^{52,53,54}

Crystals of $\text{ErSc}_2\text{N@C}_{80}\cdot\text{Co}^{\text{II}}(\text{OEP})\cdot 1.5\text{C}_6\text{H}_6\cdot 0.3\text{CHCl}_3$ and $\text{Sc}_3\text{N@C}_{80}\cdot\text{Co}^{\text{II}}(\text{OEP})\cdot 0.5\text{C}_6\text{H}_6\cdot 1.5\text{CHCl}_3$ are isomorphous. Although they differ in the content of cocrystallized solvent molecules, they have very similar arrangements of the fullerene and cobalt porphyrin components. It is remarkable that the

(47) Kobayashi, K.; Nagase, S.; Akasaka, T. *Chem. Phys. Lett.* **1996**, 261, 502.

(48) Kobayashi, K.; Nagase, S. *Chem. Phys. Lett.* **1996**, 262, 227.

(49) Takata, M.; Nishibori, E.; Sakata, M.; Inakuma, M.; Yamamoto, E.; Shinohara, H. *Phys. Rev. Lett.* **1999**, 83, 2214.

(50) Nishibori, E.; Takata, M.; Sakata, M.; Shinohara, H. *J. Synchrotron Radiat.* **1998**, 5, 977.

(51) Miyake, Y.; Suzuki, S.; Kojima, K.; Kikuchi, K.; Kobayashi, K.; Nagase, S.; Kainosho, M.; Achiba, Y.; Maniwa, Y.; Fisher, K. *J. Phys. Chem.* **1996**, 100, 9579.

(52) van Loosdrecht, P. H. M.; Johnson, R. D.; de Vries, M. S.; Kiang, C.-H.; Bethune, D. S.; Dorn, H. C.; Burbank, P.; Stevenson, S. *Phys. Rev. Lett.* **1994**, 73, 3415.

(53) Shinohara, H.; Inakuma, M.; Hayashi, N.; Sato, H.; Saito, Y.; Kato, T.; Bandow, S.; *J. Phys. Chem.* **1994**, 98, 8598.

(54) Kato, T.; Bandow, S.; Inakuma, M.; Shinohara, H. *J. Phys. Chem.* **1995**, 99, 856.

(45) Bochkarov, L. N.; Stepanseva, T. A.; Zakharov, L. N.; Fukin, G. K.; Yanovsky, A. I.; Struchkov, Yu. T. *Organometallics* **1995**, 14, 2127.

(46) Lamberts, W.; Lueken, H.; Hessner, B. *Inorg. Chem. Acta* **1987**, 134, 155.

ErSc₂N portion within ErSc₂N@C₈₀·Co^{II}(OEP)·1.5C₆H₆·0.3CHCl₃ shows the high degree of order that it does with the erbium atom localized largely on one site, a site on the crystallographic mirror plane and furthest from the cobalt atom of the porphyrin. A random distribution of the erbium ion over all three prominent metal ion sites within the C₈₀ cage seemed probable at the outset of this project, but a much higher degree of localization is observed. The most likely factor that contributes to ordering the ErSc₂N unit within the fullerene with respect to the solid-state environment outside the fullerene is the dipole moment that is created by the asymmetric ErSc₂N unit itself. The differences in electronegativity of scandium and erbium, the differences in their sizes and in the Sc–N and Er–N distances all contribute to creating this dipole.

Resolution of the disorder in the location of the C₈₀ cage in ErSc₂N@C₈₀·Co^{II}(OEP)·1.5C₆H₆·0.3CHCl₃ is particularly significant. The earlier structural work on Sc₃N@C₈₀·Co^{II}(OEP)·0.5C₆H₆·1.5CHCl₃ noted that there was an unresolved issue of residual electron density in the region of the C₈₀ cage.⁷ At the time, this electron density suggested disorder in the orientations of the C₈₀ cage, but the disorder could not be effectively modeled. However, when the disordered model used in the refinement of the ErSc₂N@C₈₀·Co^{II}(OEP)·1.5C₆H₆·0.3CHCl₃ structure is utilized in the refinement of the Sc₃N@C₈₀·Co^{II}(OEP)·0.5C₆H₆·1.5CHCl₃ structure, the *R* factor of the latter structure drops by ca. 2%, which suggests that a similar form of disorder is present in the location of the Sc₃N@C₈₀ molecule in that crystalline environment.

The *I_h* fullerene cage of C₈₀ differs significantly from that of other fullerenes that have been subject to chemical and structural characterization, because the icosahedral isomer of C₈₀ lacks any pyracylene region (Stone–Wales patch)⁵⁵ in which a 6:6 ring junction is abutted by two pentagons. In icosahedral C₈₀, the 6:6 ring junctions are abutted by a hexagon and a pentagon. As a consequence, the *I_h* isomer of C₈₀ lacks the sites that are most chemically reactive in other fullerenes, and it is likely to display distinctive chemical behavior. Similarly, the placement of the metal atoms within the *I_h* cage of C₈₀, as seen in Figures 7 and 8, may not be found in other endohedral fullerenes where pyracylene patches are present.

Experimental Section

Production of ErSc₂N@C₈₀. Graphite rods (0.25 diameter, 6 in. length) were core-drilled and subsequently packed with 180 mg cobalt oxide in a mixture of 1.0 g of graphite powder, 0.49 g of Sc₂O₃, 2.0 g of Er₂O₃ per 3.2 g of hollowed graphite rod. These rods were then vaporized in a Krätschmer–Huffman-type fullerene generator under dynamic flow of He (1250 mL/min) and N₂ (22 mL/min) to obtain samples containing ErSc₂N@C₈₀. The resulting soot from this TNT approach^{7,8} was then cold-extracted using carbon disulfide to obtain the initial endohedral extract. An NI-DCI mass spectrum of a typical ErSc stock solution is shown in Figure 1.

Separation of ErSc₂N@C₈₀. The ErSc stock solution was separated using a 3-stage HPLC approach. First, this initial extract was separated on the pentabromobenzyl, PBB, column (25 cm × 10 mm, Phenomenex Co., Torrance, CA) with CS₂ as the mobile phase. For this stage, an automated approach was utilized.²⁶ The C₈₄–C₈₈ fraction from this PBB

column was then collected and further separated with a Buckyclutter column (25 cm × 10 mm, Regis Chemical, Morton Grove, IL) using toluene as a mobile phase. Upon re-injection of the ErSc₂N@C₈₀ fraction, a single homogeneous peak was obtained. Due to coeluting impurities of this ErSc₂N@C₈₀ fraction, a third column (Buckyprep, 25 cm × 10 mm, Phenomenex Co., Torrance, CA) had to be employed. By using this Buckyprep column with toluene as the eluant, a final sample of purified ErSc₂N@C₈₀ was obtained. Its negative-ion mass spectrum and final HPLC trace are shown in Figure 2.

Crystal Growth for ErSc₂N@C₈₀·Co^{II}(OEP)·1.5C₆H₆·0.3CHCl₃: Crystals of ErSc₂N@C₈₀·Co^{II}(OEP)·1.5C₆H₆·0.3CHCl₃ were obtained by layering an orange-red solution of ca. 0.5 mg of ErSc₂N@C₈₀ in 0.5 mL of benzene over a red solution of 2.5 mg of Co^{II}(OEP) in 1.5 mL of chloroform. After we allowed the two solutions to diffuse together over a five day period, black crystals formed.

X-ray Data Collection for ErSc₂N@C₈₀·Co^{II}(OEP)·1.5C₆H₆·0.3CHCl₃: The crystals were removed from the glass tube, together with a small amount of mother liquor and immediately coated with a hydrocarbon oil on the microscope slide. A suitable crystal was mounted on a glass fiber with silicone grease and placed in the cold stream of a Bruker SMART CCD with graphite monochromated Mo K α radiation at 90(2) K. No decay was observed in 50 duplicate frames at the end of the data collection. Crystal data for ErSc₂N@C₈₀·Co^{II}(OEP)·1.5C₆H₆·0.3CHCl₃, fw = 1976.34, black parallelepiped, 0.11 × 0.03 × 0.02 mm, monoclinic, space group *C2/m*, *a* = 25.180(2), *b* = 15.0633(13), *c* = 19.650(2) Å, β = 94.791(2)°, *V* = 7427.1(12) Å³, λ = 0.71073 Å, *Z* = 4, *D_c* = 1.767 Mg m⁻³; μ (Mo K α) = 1.616 mm⁻¹; 2 Θ _{max} = 25.00°; *T* = 90(2) K; 34988 refl. collected; 6819 independent (*R*_{int} = 0.143) included in the refinement; no absorption correction performed; programs used for solution and refinement, SHELXS-97, ShelDRICK, 1990; full-matrix least-squares based on *F*², SHELXL-97; ShelDRICK, 1998; 455 parameters, 250 restraints, *R*₁ = 0.1515, *wR*₂ = 0.263 for all data; *R*₁ = 0.087 computed for 3721 observed data (>2 σ (*I*)).

The structure was solved by Patterson and difference Fourier methods. Hydrogen atoms were added geometrically and refined using a riding model. The major ErSc₂N unit, the non-hydrogen atoms of the Co^{II}(OEP) unit, and the carbon atoms of the benzene molecule with 0.50 occupancy were refined using anisotropic thermal parameters. The carbon atoms of the C₈₀ cages were refined as a rigid group utilizing ideal coordinates with *I_h* symmetry and free isotropic thermal parameters.

Note Added in Proof. The structure of Sc₃N@C₇₈ shows the Sc atoms located at the midpoints of the two carbon atoms at the center of pyracylene patches. Olmstead, M. M.; de Bettencourt-Dias, A.; Duchamp, J. C.; Stevenson, S.; Marciu, D.; Dorn, H. C.; Balch, A. L. *Angew. Chem. Int. Ed., Engl.*, in press.

Acknowledgment. This article is dedicated to Prof. Fred Wudl on the occasion of this 60th birthday. We thank the National Science Foundation (Grants CHE 9610507 and CHE 0070291 to A.L.B.) and LUNA Innovations (to H.C.D.) for support, the Gulbenkian Foundation for a postdoctoral fellowship for A.d.B.-D., and Professor R. L. DeKock and Dr. A. Tamulis for useful information. The Bruker SMART 1000 diffractometer was funded in part by NSF Instrumentation grant CHE-9808259.

Supporting Information Available: X-ray crystallographic files in CIF format for ErSc₂N@C₈₀·Co^{II}(OEP)·1.5C₆H₆·0.3CHCl₃. This material is available free of charge via the Internet at <http://pubs.acs.org>.

(55) Stone, A. J.; Wales, D. J. *Chem. Phys. Lett.* **1986**, *128*, 501.